A LOCALIZED VIBRATION RESPONSE TECHNIQUE FOR DAMAGE DETECTION IN BRIDGES

Alessio Medda and Victor DeBrunner

Department of Electrical and Computer Engineering, FAMU-FSU College of Engineering

Florida State University

ABSTRACT

Traditional techniques for damage detection in civil infrastructures that are based on the global vibration response of the system are limited in their capabilities to detect damage. Because damage detection based on the global vibration response relies on global parameters to describe the dynamic behavior of local structural elements, it suffers from limiting factors such as poorly-formed aggregate system models, very low signal to noise ratio, unrealistic boundary conditions. An alternative to the use of global detection techniques is the use of an adaptive local analysis technique based on the local response of the structure. This is achieved using wavelet packet decomposition at the sensor outputs and interpreting this decomposition as a subband framework for a bank of adaptive beamformers. The beamformer adaptive processors guaranties the maximization of the output SNR and in the same time allows for spatial selectivity and a highly directive vibration response in the structure. Scanning the structure over time produces a detailed vibration signature of the structure. The structural damage can be localized with high probability by comparing two vibration signatures before and after the damage occurs.

Index Terms— Array signal processing**,** Wavelet Packet Transforms, Subband Beamforming, Structural Health Monitoring, Damage Detection, Finite Elements

1. INTRODUCTION

Structural health monitoring (SHM) is a term used to describe a non-destructive in-situ structural evaluation method that uses any of several types of sensors which are attached or embedded in the structure. Traditional SHM techniques based on the global vibration response of the system cannot reliably predict or assess the fault present in the structure until the fault is very large. Additionally, classical SHM methods such as the ones described in the extensive literature review of Doebling *et al.* [1], based on the modification of physical properties and physical parameters, are not appropriate to the analysis of non-stationary signals such as the one from a bridge structure. A better approach to non-stationary signal analysis is through the use of functions localized in time (and space) and frequency, such as wavelet packets. The use of the wavelet packets provides a decomposition of the signal in the phase plane that yields a high frequency resolution representation of the signal. Moreover, the use of wavelet packets provides a subband framework where each sub-band signal is analyzed independently using an adaptive beamformer processor. Also, by appropriately choosing the direction of arrival of the signal it is possible to achieve spatial selectivity on the structure and a highly directive vibration response. The validation of the method is done using finite elements to approximate the dynamic behavior of the structure. The comparison between the vibration response of an undamaged and a damaged simulated structure reveals that the simulated damage is localized in frequency in the direction of the damage. An extensive version of this work is presented in [2]. Because the propose approach requires observations from an excited bridge, the damage will be detected as long as the external traffic provides a broad spectrum excitation. This statistically base premise implies that for some traffic conditions the method can deliver false detections. This problem can be easily resolved considering a cumulative map, where the result of the detection is recorded in intensity e position over time. This decision process is shown in Figure 1.

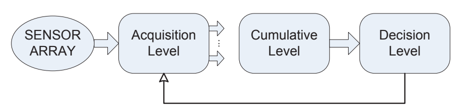

Figure 2. Conceptual diagram of the decision process associated with damage detection.

Also, this work is closely related with the results presented in [9] by Hieu *et al.*, where real data from a in-service highway bridge is used for system identification of the structure.

2. SUBBAND FRAMEWORK

The vibration signals found in a structure such as a highway bridge are non-stationary and they are not well-suited to be analyzed with standard frequency estimation techniques. The use of wavelet packets provides a phase-plane representation of the signal with good high frequency resolution, and represents a good solution for the analysis of non-stationary signals of this kind [3]. Moreover, the wavelet packet decomposition provides a good subband framework that allow for the use of subband techniques, such as subband beamforming on a broadband signal [4]. Because the signal impinging on the sensors is a broadband signal and does not satisfy the narrowband condition, there is the need to divide the signal acquired by each sensor into small frequency bands, where the narrowband assumption is viable. Processing each sensor output with a wavelet packet filter bank, the sensor signal is divided in $B = 2^L$ sub-bands, where L is the depth in the wavelet packet decomposition. Each frequency band is characterized by its center frequency f_c, characteristic of the mother wavelet used for the analysis. Therefore, the signal in each subband satisfies the narrowband condition as described in [5], providing the conditions to use an adaptive beamformer on each sub-band. Since the total number of beamformers is equal to B, the b^{th} beamformer receives in input the signals from sensor 0 to $N-1$ but only from the b^{th} subband, where $b = 1,2, \dots B$. Each beamformer is tuned to the subband center frequency – this means that for a given direction of arrival, the sensor delays are computed based on f_c.

2.1 Nearfield adaptive beamformer

Vibration analysis in a vibroacoustic environment such as a highway bridge assumes the sensors to be placed directly on the vibrating structure. That is, if we consider the sensors on the bottom of a girder, the input to the system is the random traffic on top of the deck, and the vibration is the propagating vibration generated by the traffic on the structure. Because the range of frequency considered goes from 0Hz to 128Hz, being 256Hz the sampling frequency, the source can be considered to be in the nearfield. This is equivalent to have the source in the Fresnel zone of the array, or $0.62(L_r{}^3/\lambda) < |\vec{k}| < 2L_r{}^2/\lambda$. Here L_r is the aperture of the array, $|\vec{k}|$ is the distance of the source form the array reference point and λ is the wavelength. Therefore, the farfield assumption (source at infinite distance with propagating plane waves) cannot be used and a compensation for the nearfield distortion must be adopted. This situation is illustrated in Figure 2, where only half of the beam of length L is represented in vertical orientation, to simplify the explanation. The sensors are placed at the bottom of the beam, and are represented by the red dots. The source is on the top of the beam and the propagating wave front is spherical. The phase shift associated with the propagation time delays can be computed from the difference $|\vec{k}_n| - |\vec{k}|$, as

$$\tau_n(\vartheta_0) = \frac{|\vec{k}_n| - |\vec{k}|}{\sigma} \quad n = 0, \dots N-1 \tag{1}$$

where $|\vec{k}_n|$ is the distance between the source and the n^{th} sensor. The correction for spherical propagation and the distance attenuation can both be incorporated using a compact description of the geometric properties of the array. A vector that incorporates these properties is the *array propagation* vector $\mathbf{D}(\omega, \vartheta)$ defined as

$$[\mathbf{D}(\omega, \vartheta_0)]_n = \alpha_n(\vartheta_0) e^{j\omega \frac{|\vec{k}_n(\vartheta_0)| - |\vec{k}(\vartheta_0)|}{\sigma}} \qquad n = 0, \dots N-1 \tag{2}$$

where $\alpha_n(\vartheta_0) = |\vec{k}_n(\vartheta_0)| / |\vec{k}(\vartheta_0)|$ takes into account he attenuation due to the distance from sensor and source emitter. Consequently, it can be defined a *compensation vector*, that allows the array to be steered in different directions. The compensation vector is defined as the reciprocal of the array propagation vector

$$[\mathbf{H}^T(\omega, \varphi)]_n = \frac{1}{\alpha_n(\varphi)} e^{-j\omega \frac{|\vec{k}_n(\varphi)| - |\vec{k}(\varphi)|}{\sigma}} \tag{3}$$

so that only when $\varphi = \vartheta_0$ the compensated nearfield response is identical to the farfield response. For angles close to ϑ_0, the two responses are approximately equal. Figure 3 shows the comparison between the desired far-field (solid line), the near-field uncompensated (dash-dot line) and the near-field compensated (dashed line) beampattern response. The near-field uncompensated beampattern response is the beampattern obtained using a farfield assumption when the signal is in the near-field. The near-field compensated beampattern response is obtained using equation (3). The beamformer output for a narrowband source may be written as

$$\begin{aligned} y(t) = \mathbf{S}_{2K+1}{}^T & \left[\mathbf{W}^T \operatorname{diag}\left(\mathbf{H}^T(\omega, \varphi)\right) \mathbf{D}(\omega, \vartheta_0)\right] \\ & + \mathbf{N}_{2K+1}{}^T [\mathbf{W}^T \mathbf{H}^T(\omega, \varphi)] \end{aligned} \tag{4}$$

with $\mathbf{S}_{2K+1} = [f(t+K) \dots f(t) \dots f(t-K)]$ the input vector and $\mathbf{N}_{2K+1} = [\nu(t+K) \dots \nu(t) \dots \nu(t-K)]$ the noise vector. The matrix of complex weights is defined as

$$\begin{aligned} \mathbf{W} &= [\mathbf{w}_{-K} \dots \mathbf{w}_0 \dots \mathbf{w}_K] \\ &= \begin{bmatrix} w_{0,-K} & \cdots & w_{0,0} & \cdots & w_{0,K} \\ w_{1,-K} & \ddots & w_{1,0} & \ddots & w_{1,K} \\ \vdots & & \vdots & & \vdots \\ w_{N-1,-K} & \cdots & w_{N-1,0} & & w_{N-1,K} \end{bmatrix} \end{aligned} \tag{5}$$

The adaptive processor needs to update the time varying filter coefficients for every new set of inputs. The adaptation is done using the classical Griffiths and Jim [6] adaptive processor.

2.2 Minimum angle discrimination

To obtain a highly directive vibration response, we adjust the direction of arrival of the sensor array, steering the beam in the direction of interest. The minimum angle separation between two scanning directions is the *angular resolution* of the array. Because each beamformer in the subband architecture is operating at a difference frequency, the angular resolution is not constant, and it can be expressed as

$$\alpha_{min} = \frac{180}{\pi} \frac{\lambda_c}{L_r} \tag{6}$$

where $\lambda_c = \sigma_0 / f_c$ is the wavelength related to the frequency of operation f_c, with σ_0 speed of propagation in the medium. Equation (6) indicates that the resolution increases with frequency. At low frequencies, the beampattern is wide and it rolls-off slowly, and it is therefore not possible to achieve high directivity. One cannot increase the number of scanning angles at low frequencies because the resulting beampattern will be spatially aliased. Restricting the beam scanning as in Equation (6) produces no aliasing. Consequently, we should scan the structure using variable spatial resolutions according to the frequency.

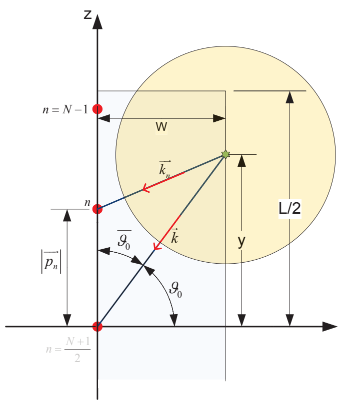

Figure 2. Nearfield propagation of a monochromatic wave in a finite beam of length L and width W.

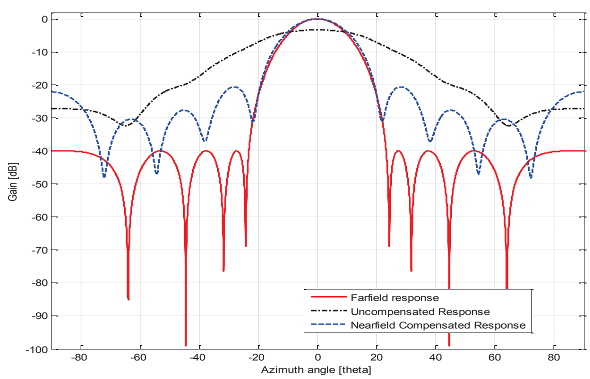

Figure 3. Comparison of far-field, uncompensated near-field and compensated near-field beampattern response for an array of 9 sensors, using Chebyshev 40 dB weights and $d/_{\lambda} = 0.5$.

3. DAMAGE DETECTION

It is known that damage inside the structure, like a crack or a localized delamination, changes the way the signal is propagated. It is also known that this type of change has been associated with energy variation [7]-[8]. Wavelet packet energy can be used, and it is defined as

$$\mathrm{E}_{\Omega_\ell} = \sum_{n} \left(Y_{\Omega_\ell}(n)\right)^2 \tag{7}$$

where $Y_{\Omega_\ell}(n)$ represents the signal at the output of the ℓ^{th} beamformer for the angle Ω_ℓ, where $\ell \in [1, 2^L]$. Changes in energy and in its distribution are only measurable with a comparison between two complete energy profile scans of the structure. Therefore, each scan needs to be representative of a state of the system so that their difference will highlight the changes in the energy distribution due to the event (damage) occurring between the measurements. Also, the change occurred in the structure between two different scans can be associated with an event that alters the internal configuration of the system, like a crack that propagates, corrosion in the structure or delamination. Under these circumstances, it is possible to measure the difference in the energy distribution using the metric $\mathrm{D}_{\Omega_\ell} = \left|\mathrm{E}_{\Omega_\ell}^{\mathrm{DMG}} - \mathrm{E}_{\Omega_\ell}^{\mathrm{UND}}\right| \cdot \mathrm{E}_{\Omega_\ell}^{\mathrm{UND}}$, where the subscripts DMG and UND refer to the two states (damaged and undamaged, respectively) of the system.

4. SIMULATION RESULTS

A simple simulation of the proposed method is done using a Finite Element approximation of a simply supported beam. The simulated beam is 100 ft in length, approximated with 500 elements with a cross section of 1500 in^2 and a mass density of 150 lb/ft^3. The response of the beam is obtained exciting the structure with a sequence of three simulated triaxial trucks at constant speed of 20 mph, 30 mph and 40 mph, sequentially crossing the beam. The trucks have a single mass of 40,000 lb. Details on the Finite Element model used can be obtained in [2] and its references. Two versions of the beam are simulated. The first simulated beam contains no damage and the second simulated beam has a damage placed at 54 ft from the beginning of the beam, centered at element 270. The damage is simulated reducing Young's modulus of the damaged element and depending on the severity of the damage also the surrounding elements are interested. In our case the damage goes from element 268 to element 272. In the simulation 300 virtual sensors are used, with a sensor spacing of 4 inches. The maximum number of scanning angles is 338 and is obtain at the Nyquist frequency with $\alpha_{min} = 0.45°$. The wavelet packet decomposition is implemented using a Daubechies 7 mother wavelet at decomposition level 7, generating 128 subbands. The damage is localized between the 16° and 20° angles. The analysis of the differential energy at the beamformer output can only be correctly evaluated if we restrict the frequency axis to limited windows. The plot of the all frequency spectrum is masked from the energy differences contains in the first subbands, where all the energy is concentrated in few scans. In order to see the fine details, it is necessary to slice the plot along the frequency axis and analyze each section separately. Figure 4 shows the differential energy map for the 30 Hz to 60 Hz range and Figure 5 shows the frequency range from 80 Hz to 128 Hz. In both plots the local features emerge in form of local maxima, localized around the direction of the damage for localized subband frequencies. The damaged locations identified are at 14° and 21° for Figure 4 and 16° and 20° for Figure 5, both directions that are associated with damage. The maximum at 39° is explained by the fact that for angles past the damage location, the beampattern is still measuring part of the response from the damaged zone because of how the Finite Element model is built. Because the separate analysis of the differential energies can be slow and cumbersome, an automatic damage location procedure is required. A simple solution is to account for all the local maxima and their locations after the higher energies in the lower part of the spectrum are removed. Using a non overlapping sliding window, every location at each sub-band central frequency is accounted for its angular position. The result is then incrementally added to a vector. The resulting normalized pseudo density is shown in Figure 6, where the maximum of the distribution is located around 20°, identifying the location with higher damage probability.

CONCLUSIONS

This work presents a Structural Health Monitoring technique that combines well-known signal processing methods in a new framework. Thanks to the use of the wavelet packet to isolate the sub-band components of the acquired signal and the employment of near-field beamforming techniques to optimal filter and spatially sample the structure, it is possible to analyze the vibration signal for direction of arrival and frequency components.
Because of the nature of the damage that is investigated and the nature of the proposed solution to the problem, the identification of the damage is possible only through a comparison of different time states of the structure. This change is reflected in the energy distribution of the structure, and can be identified using a simple normalized energy difference. The results from the validation analysis suggest that the damage is localized in frequency and space and the angles influenced by the damage are those in the direction of the damage, with small exceptions, probably because of the imperfection of the used model.

REFERENCES

[1] S. W. Doebling, C. R. Farrar, and M. B. Prime, "A Summary Review of Vibration-Based Damage Identification Methods," *The Shock and Vibration Digest*, vol. 30, n. 2, pp. 91−105, 1998.

[2] A. Medda and V. DeBrunner, "Near-Field Sub-band Beamforming for Damage Detection in Bridges," *Structural Health Monitoring, and International Journal,* to be published.

[3] S. Mallat, *A Wavelet Tour of Signal Processing 2nd edition*, Academic Press, 1999.

[4] F. Lorenzelli, A. Wang and K. Yao, "Broadband array processing using subband techniques," *Acoustics, Speech, and Signal Processing, ICASSP-96 Conference Proceeding*, vol. 5, pp. 2876−2879, 1996.

[5] H. L. Van Trees, *Detection, Estimation, and Modulation Theory, Part IV: Optimum Array Processing*, Wiley and Sons, New York, 2002.

[6] L. Griffiths and C. Jim, "An alternative approach to linearly constrained adaptive beamforming," *IEEE Transactions on Antennas and Propagation*, vol. 30, no. 1, pp. 27−34, 1982.

[7] Z. Sun and C.C. Chang, "Structural damage assessment based on wavelet packet transform," *Journal of Structural Engineering,* vol. 128, no. 10, pp. 1354–1361, 2002.

[8] S.S. Law, X.Y. Li, X.Q Zhu and C.C. Chan, "Structural damage detection from wavelet packet sensitivity," *Engineering Structures,* vol. 27, no. 9, pp. 1339–1348, 2005.

[9] H. Thai, V. DeBrunner, L. DeBrunner, J.P. Havlicek, K. Mish, K. Ford, A. Medda, "Deterministic - Stochastic Subspace Identification for Bridges," *IEEE/SP 14th Workshop on Statistical Signal Processing*, pp.749-753,. 2007.

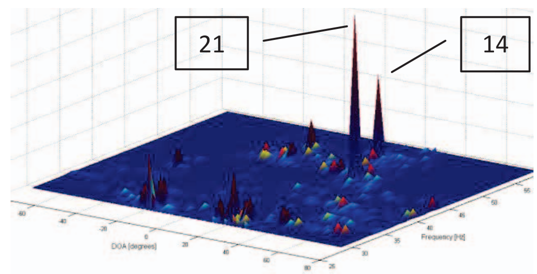

Figure 4. Differential Energy map for the region between 30 Hz and 60 Hz. Artifacts are present at location in proximity of the simulated damage.

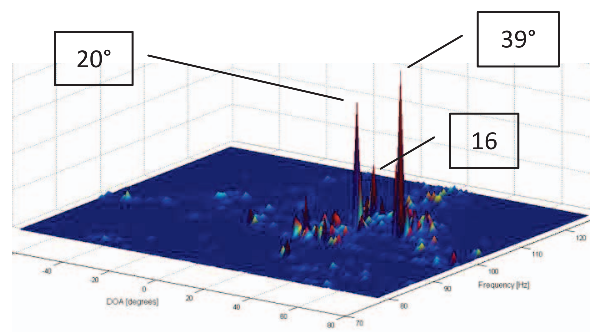

Figure 5. Differential Energy map for the region between 80 Hz and 128 Hz. A higher resolution implies more details, with more artifacts in the proximity of the damage location.

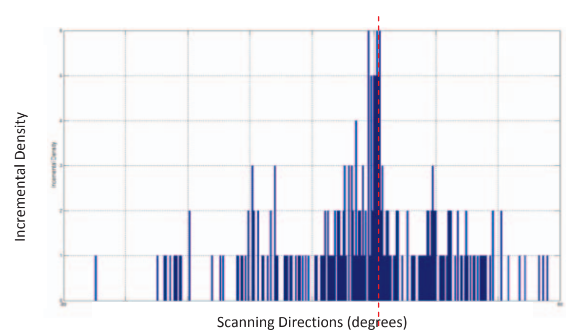

Figure 6. Pseudo-incremental density. The peak for 20° indicates the direction with higher damage probability**.**